A Review on Stability Analysis Methods for Switching Mode Power Converters

Abdelali El Aroudi, *Senior Member, IEEE*, Damian Giaouris, Herbert Ho-Ching Iu, *Senior Member, IEEE*, and Ian A. Hiskens, *Fellow, IEEE*

***Abstract*—In distributed power generation systems a pivotal role is played by DC-DC power converters that are employed to connect local loads to local power sources. These converters are used either in combinations of series/parallel connections or as stand-alone devices. A lot of work has taken place in the stability analysis of these converters and several methods have been used/proposed with different properties, strengths and weaknesses. Describing all existing methods is probably a never ending task and therefore in this tutorial paper four different methods will be presented by pointing out their main properties and explaining briefly how they can be used in applications that involve power converters. More specifically, the chosen methods are based on 1) the Poincaré map, 2) Saltation matrix, 3) trajectory sensitivity, and 4) steady-state-response analysis of the discrete-time model. Simple case studies from previous publications are collected and presented in order to further explain these methodologies. Finally, this paper intents to describe some of the future challenges that exist in the area of stability analysis of power converters especially when these are employed in distributed generation applications.**

***Index Terms*—DC-DC converters, distributed power systems, Poincaré map, Saltation matrix, stability analysis, steady state analysis, trajectory sensitivity.**

I. Introduction

A. Distributed Generation Systems

DISTRIBUTED Power Generation (DPG) systems are considered one of the key aspects of tomorrow's power grids. Their main characteristic is the ability to locally produce and distribute energy with high efficiency. Furthermore, by using Renewable Energy Sources (RESs) it is possible to offer a more environmental friendly approach and to greatly reduce the emissions of harmful gasses into the atmosphere [1]. Finally, due to the local nature of such systems it is possible to avoid using AC transmission and to employ DC operation. Another advantage that is associated with DPG systems is the ability to use microgrids, i.e., to combine several local energy storage facilities (like batteries and hydrogen tanks), a number of power sources (like photovoltaic panels and fuel cells) and a set of local loads without the necessary requirement to connect to the main power grid. Hence, apart from the improved efficiency that the DPG systems offer, a microgrid provides better control, monitoring, fault detection/isolation and power quality. When the microgrid concept is applied to residential electrical systems, at the low power level (10–100 kW), it is called a nanogrid [2]. Combining net-metering, communications, and remote control such nanogrids could become building blocks of the so called *smartgrid* [3].

All DPG topologies require specific power electronics modules to convert the generated power into a regulated one that can be directly interconnected with the utility grid and/or can be used to supply the consumer loads [4]. In order to exploit the power that is locally produced and to satisfy the demand of various local loads, it is necessary to use several DC-DC converters at various power levels. The quality and efficiency of the overall system is therefore tightly connected to the operation of these power converters. The main requirements for the satisfactory performance of power converters are 1) operation at the desired voltage/current level, 2) minimization of any AC components in the system (ideally only a single DC component should be present), 3) the minimization of the current/voltage ripple that can greatly decrease the efficiency/life time of the converter and 4) fast response in the presence of load/source changes and other external disturbances.

B. Nonlinear Phenomena in Switching Converters

Switching mode power converters employ electronic switches (such as diodes, IJBTs, MOSFET, and others) to deliver a regulated current/voltage. When these switches are required to be controlled, an external clock is used and therefore the only acceptable nominal operation of any DC-DC converter is a periodic oscillation around the desired level, i.e., apart from a DC component, there always exists an AC component at the frequency of the clock. This nominal behavior is also called period-1 operation and the resulting vector field that describes the converter is nonsmooth due to the switching action. When the stability of this periodic operation is lost the converter either operates at a different undesired voltage/current level or

Manuscript received March 29, 2015; accepted July 02, 2015. Date of publication August 25, 2015; date of current version September 09, 2015. This work was supported the Ministerio de Ciencia e Innovación under Grants DPI2013-47293-R and CSD2009-00046 and the Department of Electrical Engineering of The Petroleum Institute, Abu Dhabi, UAE . This paper was recommended by Guest Editor M. Delgado-Restituto.

A. El Aroudi is with the GAEI Research Center, Departament d'Enginyeria Electrònica, Elètrica i Automàtica, Escola Tècnica Superior d'Enginyeria, Universitat Rovira i Virgili, 43007 Tarragona, Spain (e-mail:abdelali.elaroudi@urv.cat).

D. Giaouris is with Chemical Process Engineering Research Institute, Centre for Research and Technology Hellas, 570 01 Thermi-Thessaloniki, Greece (e-mail: giaouris@cperi.certh.gr).

H. H.-C. Iu is with the University of Western Australia, Perth 6009,Australia (e-mail: herbert.iu@uwa.edu.au).

I. A. Hiskens is with the University of Michigan, Ann Arbor, MI 48109 USA (e-mail: hiskens@umich.edu).

Color versions of one or more of the figures in this paper are available online at http://ieeexplore.ieee.org.

Digital Object Identifier 10.1109/JETCAS.2015.2462013

extra frequency components are present or we have a dramatic increase of the current ripple [5], [6]. Therefore, the stable behavior of the nominal periodic motion is of paramount importance for the proper operation of the converter and hence of the overall system. The transition from a stable to an unstable operation is called a bifurcation and it is possible to have three different types in relation to the aforementioned criteria.[1]

- Neimark-Sacker (NS) bifurcation that creates extra high amplitude low frequency AC components.
- Saddle Node (SN) bifurcation that may force the converter to operate at undesirable voltage/current level.
- Period Doubling (PD) bifurcation and the associated subharmonic oscillation that leads to an increase in the current ripple.

The occurrence of any of the above phenomena can have a damaging affect on the converter and the devices that it interconnects. Therefore, the stability analysis of the converter's nominal periodic motion is crucial for the overall operation of the system and a lot of work has taken place on producing tools that will allow a power electronics engineer to predict when these bifurcations will occur, what is the underline mechanism for their creation and also how they can be avoided. In the next subsection, some of these methods will be briefly described and then better analyzed in Section II.

C. Literature Review and Brief Presentation of the Main Stability Analysis Methods

The stability analysis of switched mode power converters was originally tackled by using their averaged models [7], [8] where the periodic operation of the converter is ignored and the resulting nonlinear model is linearized around the operating point. More specifically, a great effort has been made in the last three decades on obtaining design-oriented averaged models for switched converters and many types of these models exist in the relevant literature. Even though these averaged models can describe the low frequency or slow scale dynamics of switching converters, unfortunately they cannot predict all the nonlinear phenomena that can be observed in such systems since they ignore the main source of nonlinearity, namely, the switching action and the associated induced ripple in the state variables. Therefore, since the pioneering works of Middlebrook andČuk [8] in the seventies, there have been proposed many improvements in order to take into account these peculiar phenomena that cannot be predicted by conventional averaged models. More specifically, to include the effect of the switching action, "enhanced" averaged models have been suggested [10], [11] that can predict the stable operating area. Also, in [12] a zero order hold transfer function is included to take into account the sampling effect of the modulator while [13] uses a general modelling method based on the Krylov–Bogoliubov–Mitropolsky ripple estimation technique. Unfortunately all these modelling approaches greatly depend on the converter topology and the controller that is being used [13], [14] and therefore they cannot be generalized and used in all cases. Apart from predicting the stability boundaries, averaged models have also been used to design controllers mainly after a local linearization and by applying linear design techniques such as Bode, Nyquist, and root-locus plots or by directly using modern state-space (both linear and nonlinear) methods [15]. Finally, more advanced control algorithms such as robust and optimal control techniques have also been developed based on these models [16]–[18]. For interconnected switching converters Middlebrook andČuk [19] suggested, in the 1970s, the Minor Loop Gain (MLG), namely the ratio of the output impedance of the source converter to the input impedance of the load downstream converter as simple tool for stability analysis. A review of the stability criteria using the previous approach can be found in [9]. Unfortunately this approach cannot unfold all the internal fast-scale nonlinear dynamics of the system and the associated complex interaction between the source and the load converters.

On the other hand, instabilities at the fast switching time scale (i.e., PD bifurcations) that produce subharmonic oscillations, have been reported in the early seventies in studies dealing with the analysis of efficient switched mode power supplies under PWM operation [20]. Realizing that PD bifurcations and the associated subharmonic oscillation cannot be completely predicted by the aforementioned standard stability analysis tools, discrete-time models were employed. The discrete-time models are obtained by sampling the exact system state-space representation at the switching period. This is equivalent to placing a surface in the state space in such a way that the continuous orbit is represented by a map (that is called the Poincaré map) on that surface. Then the eigenvalues of the Jacobian matrix of the Poincaré map evaluated at that fixed point determine the stability of the periodic orbit [21]. This matrix of the Poincaré map is also called Monodromy matrix and its eigenvalues are called Floquet multipliers. The discrete-time models attracted a lot of interest initially by Prajoux *et al.* [22] then continued by Lee and Yu [23] and later by Verghese *et al.* [24].

By the end of the 1980d, Hamill and Deane extended the study of the fundamental periodic orbit and analyzed various bifurcation and chaotic phenomena [25], [26] that are present in switched mode power converters. Since then a lot of work has taken place (see [5], [6], [27]–[29] and the references therein) and the Poincaré map was derived for numerous power converter topologies with multiple configuration structures [32] and various exotic nonlinear behaviours were studied.

In general, discrete-time models or maps are widely used to study bifurcations in DC-DC converters and for their digital control design [30], [31]. They have been successfully applied in voltage-mode controlled buck converters [33] and current-mode controlled boost converters [37]. Furthermore, PD and other bifurcations causing the formation of solutions in the high-frequency range can be studied through appropriate discrete-time models not only for converters with a reduced number of configurations [26], [29], [34] but also those characterized by multiple number of configurations such as paralleled [35], cascaded [36] and multi-cell converters [32]. An extensive literature repository already exists with methods of analysis and classification of standard bifurcations like PD and Hopf (or Neimark-Sacker) bifurcations [21]. Finally, through the usage of the discrete time models it is possible to predict and

[1]Another type of bifurcation is also possible here, the so-called border collision or discontinuity induced bifurcation. However this will not be presented in this review.

hence avoid these instabilities that can greatly downgrade the performances.

While the Poincaré map, as it was originally proposed, can theoretically be derived for any power converter and operating mode (even if not in closed form), it becomes cumbersome when used in complicated cases that involve several switching topologies (like parallelly connected, interleaved, resonant or multi-cell converters). This is mainly because the switching action depends on the original perturbation that is placed on the map in order to produce its Jacobian matrix. Another approach is to effectively ignore this dependance and to include in the derivation of the Jacobian, a "correction" map. Even though this may seem more complicated for simple DC-DC converters, it greatly simplifies the overall analysis and more importantly through this simplification the resulting model can be used for design purposes as it will be better explained later in the paper. The structure of this correction map depends on the smoothness and continuity of the vector fields. Filippov [38] in 1988 suggested the Saltation matrix for systems that have nonsmooth but continuous vector fields while Nordmark and Dankowicz [39] in 1999 proposed the Discontinuity Map for systems that involve jumps in the state space[2]. These two methods were first applied in mechanical systems and a more detailed analysis can be found in [28], [40], [41]. In electrical systems it is not possible to have jumps in the state space and therefore the Saltation matrix was used in 2008 [42] to study the nonlinear behavior of a voltage controlled buck converter. Furthermore, because in DC-DC converters the vector fields before and after each switching are linear, this approach allowed a more systematic representation of the Jacobian matrix and hence the study of more complicated converter topologies [43]–[49].

Trajectory sensitivities provide an alternative view of the perturbation analysis underpinning Floquet theory and Saltation matrix concepts. In particular, trajectory sensitivities are motivated by truncating the Taylor series expansion of the flow (or orbit) and describe the change in a trajectory resulting from perturbations in initial conditions and parameters. It is shown in [50] that trajectory sensitivities are well defined for hybrid dynamical systems where the flow is determined by differential-algebraic equations, and discrete events incorporate arbitrarily complicated switching conditions and state reset (jump) actions. Trajectory sensitivities are described by variational equations along smooth sections of an orbit, and can be computed as a by-product of numerical integration if an implicit integration technique is used to generate the flow. Their evaluation at switching events is described by the Saltation matrix. Evaluating trajectory sensitivities over a limit cycle gives the Monodromy matrix that describes the stability properties of the limit cycle. Trajectory sensitivities provide gradient information required by shooting methods for solving boundary value problems such as locating limit cycles.

All the previous techniques can be classified as dynamical approaches and lead to the same expression of the Jacobian matrix of the switched system in the discrete-time domain. After obtaining this matrix, critical boundary conditions for singularities like SN bifurcation or PD can be obtained by imposing in the characteristic equation that one of the eigenvalues is equal to $+1$ or -1, respectively [51].

Another approach used for the first time in [51] for locating PD bifurcations in a buck converter is by using a Fourier series expansion of the steady-state feedback signal and then to impose specific conditions that occur when a PD takes place. The frequency-domain expression that was first derived in [51] has been recently re-considered in [52] and [53] arriving to closed form expressions for the boundary of subharmonic oscillation in the time domain. In [52] and [53], the transformation from the Fourier frequency-domain to the time-domain is based on using the *transfer function* of switching converters with linear plants. However, most of the switching converters are bilinear and this transfer function cannot be directly defined without averaging. Based on that approach another methodology was proposed in [54] where now the steady-state feedback signal is directly analyzed in the time domain and easy-to-use critical instability boundary expressions corresponding to SN and PD bifurcations for the general case of bilinear DC-DC converters have been obtained.

In this paper the previously mentioned techniques for predicting instabilities in switching converters are presented. It has to be stated here that other methods have also been proposed with various advantages and disadvantages. For example in [34] a similar expression as the monodromy matrix was derived from discrete-time analysis while two very powerful methods have been proposed in [55], [56]. However, due to space limitations only the dour aforementioned methods will be described.

The rest of the paper is organized as follows. Section II briefly presents the mathematical switched model of power electronics circuits. The discrete-time model in the form of a Poincaré map is presented in Section III. In Section IV, the Floquet theory and the Saltation matrix as applied to DC-DC converters are explained. The trajectory sensitivity approach is detailed in Section V. An approach based in steady-state analysis in the time domain is presented in Section VI. Some examples of power electronics converters are used in Section VII to illustrate the use for the previous techniques for stability analysis and for prediction of the instability boundaries in the parameter space. Finally some concluding remarks and future challenges are discussed in the last section.

II. Mathematical Model of a DC-DC Converter

As it has been previously stated, DC-DC converters employ switches that periodically change their configurations resulting in a switched system. Due to the presence of switches, the dynamical model of the system is given by a piecewise function that depends on the location of the system's trajectory in the state space. Suppose the switching converter under study toggles between N circuit topologies. In one switching cycle, it spends a fraction of time in each particular topology. Let x be the state vector, d_j be the fraction of the period in which the circuit stays in the jth topology, and T be the period of one switching cycle. Obviously, we have $d_1 + d_2 + \cdots + d_N = 1$. The general

[2]Obviously if the vector fields are continuous but nonsmooth both methods result in the same correction map.

nonsmooth dynamical model of the converter is

$$\dot{x} = f(x,t,\rho) = \begin{cases} f_1(x,t,\rho), & \text{for } x \in R_1 \\ f_2(x,t,\rho), & \text{for } x \in R_2 \\ \vdots & \\ f_N(x,t,\rho), & \text{for } x \in R_N \end{cases} \quad (1)$$

where $R_1, R_2, \ldots R_N$ are different regions of the state space, separated by $(N-1)$ dimensional surfaces given by algebraic equations of the form $h_i(x,t) = 0$, $i = 1 \ldots N-1$ called "switching manifolds". When the circuit configurations used by the converter are linear, we can write down the following state equations for each clock cycle:

$$\dot{x} = \begin{cases} A_1 x + B_1 w, & \text{if } 0 \le t < d_1 T \\ A_2 x + B_2 w, & \text{if } d_1 T \le t < (d_1+d_2)T \\ \cdots & \\ A_N x + B_N w, & \text{if } (1-d_N)T \le t < T \end{cases} \quad (2)$$

where A_j and B_j are the system matrices for the jth topology and w is the vector of external input parameters. It should be noted that usually practical switching converters involve a relatively small N.

III. Poincaré Map

This section presents one of the most commonly used modelling approaches for bifurcation analysis, i.e., the discrete-time iterative-map approach. The derivation of iterative maps is relatively complicated but the resulting models offer a complete information on the dynamical behavior of the system under investigation. This approach is able to predict low frequency (slow-scale) and high-frequency (fast-scale) nonlinear phenomena [5].

Basically, the aim is to derive an iterative function that expresses the state variables at one sampling instant in terms of those at an earlier sampling instant. To illustrate the idea, we consider maps obtained by uniform sampling of the system states at time instants multiple of the period T, i.e., $t = nT$, for $n = 0, 1, 2, \ldots$. As the vector fields between the switching events are linear (2) we can use the fundamental theorem of calculus to express the value of the state vector at the end of the subinterval corresponding to the jth topology in terms of its value at the beginning of that subinterval, Fig. 1. For brevity, let t_j be the time instant at the beginning of the jth subinterval, i.e., the time instant that corresponds to the circuit switching from the $(j-1)$th to the jth configuration. Moreover, letting d_j be the duty ratio corresponding to the subinterval beginning at t_j, i.e., $d_j = (t_{j+1} - t_j)/T$, we have

$$x(t_{j+1}) = \Phi_j(d_j T)x(t_j) + \Psi_j(d_j T) \quad (3)$$

where $\Phi_j(t) = e^{A_j t}$ and $\Psi_j(t) = \int_0^{d_j T} \Phi_j(s) B_j w ds$. By composing together equations for all subintervals within a switching period, we obtain the following iterative map:

$$\begin{aligned} x_{n+1} &= P(x_n, d_n) \\ &= \Phi_T(d_1, d_2, \ldots)x_n + \Psi_T(d_1, d_2, \ldots) \\ h(x_n, d_n) &= 0 \end{aligned} \quad (4)$$

where $h = (h_1, h_2, \ldots)^\intercal$ is the vector of functions defining the switching manifolds, x_n denotes the state vector at $t = nT$, d_n denotes the set of duty ratios for the cycle beginning at $t = nT$, i.e., $d_n = (d_1, d_2, \ldots . d_N)^\intercal$ [32]

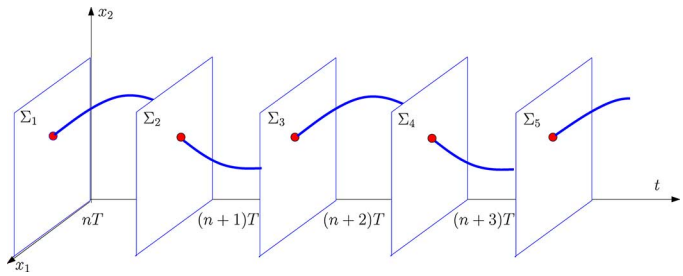

Fig. 1. Partitioning the state space into different regions. In each region the system is described by a distinctive flow.

$$\Phi_T(.) = \prod_{k=N}^{1} \Phi_k(d_k T) \quad (5a)$$

$$\Psi_T(.) = \sum_{j=1}^{N-1} \prod_{k=N}^{j+1} \Phi_k(d_k T)\Psi_j(d_j T) + \Psi_M(d_N T). \quad (5b)$$

Once the discrete-time map has been derived, and its fixed point that corresponds to the original periodic motion found, it is possible to calculate its Jacobian by [7], [32]

$$J = \frac{\partial P}{\partial x_n} - \frac{\partial P}{\partial d_n}\left(\frac{\partial h}{\partial d_n}\right)^{-1}\left(\frac{\partial h}{\partial x_n}\right). \quad (6)$$

Then the stability of the fixed point is determined by calculating the eigenvalues of the Jacobian through

$$\det|\lambda I - J| = 0. \quad (7)$$

The eigenvalues of the Jacobian matrix determine not only the stability of the periodic orbit but also the three aforementioned bifurcation scenarios, Fig. 2. In Fig. 2(a) a stable (node) and an unstable (saddle) limit cycle (shown in the bifurcation diagram as fixed points) collide and are annihilated. Prior to the bifurcation the stable fixed point has one real eigenvalue smaller than 1, while the saddle has one real eigenvalue just greater than 1. As we approach the bifurcation point, these two eigenvalues approach each other and at the bifurcation boundary they both become 1. A different scenario is observed in Fig. 2(b) where a stable period 1 orbit losses stability (but it continues to exist as unstable) and a period 2 orbit is created with much bigger size (i.e., when it occurs in a DC-DC converter we have a sudden increase of the current ripple). In this case the stable period 1 orbit has one real eigenvalue that becomes -1 at the bifurcation point and when the period 2 is born it has one eigenvalue at 1. Finally, in Fig. 2(c) the stable period 1 orbit loses stability (as in case b) but now a quasi-periodic orbit (i.e., a torus) is created. Now, we have two complex eigenvalues with magnitude greater than 1 [21].

Many analytical results and solution approaches can be found in standard texts on nonlinear dynamical systems that can be modelled by iterative maps [21], [28], [55].

IV. Saltation Matrix

Another tool for accurate stability analysis of switching converters without going through discrete-time modelling is

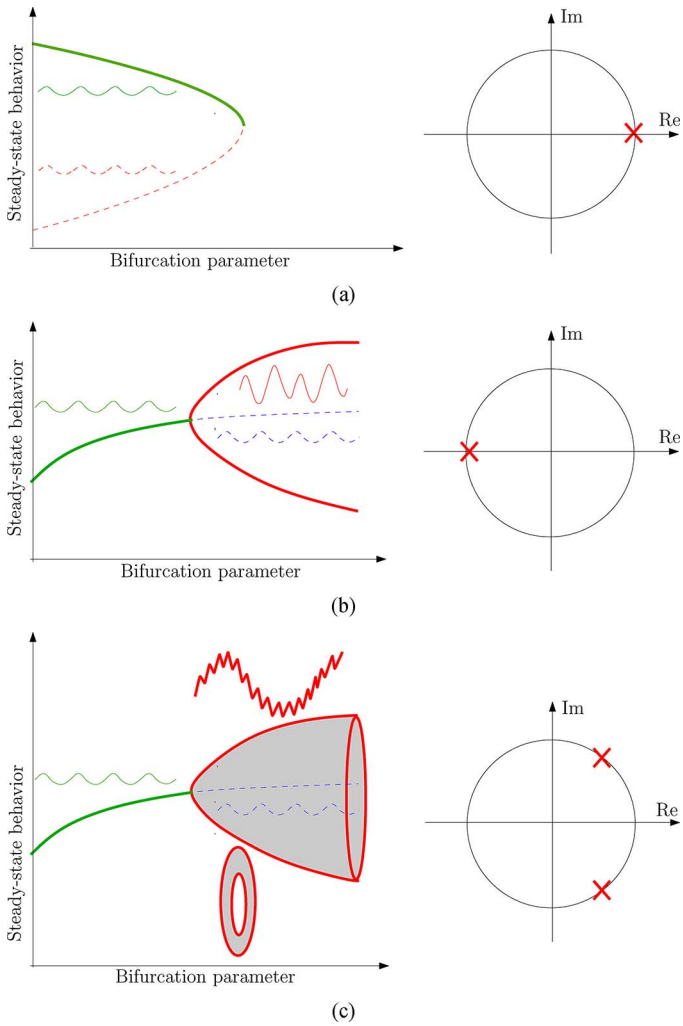

Fig. 2. On the left: Bifurcation scenarios showing the three basic instabilities that can occur in a periodic orbit. The solid trace denote stable and the dashed unstable orbits. On the right: The unit circle and the location of the eigenvalues of the period 1 orbit in each case at the onset of instability.

by using Floquet theory and Filippov's method. In this section we will present the idea behind this approach and how this can be used for stability analysis of the nominal operation of the periodic orbits that appear in power converters. Prior to that, we have to see the basic concepts of stability theory for smooth dynamical systems and what are the main problems when applied to switched systems.

A. Smooth Orbits

The stability of a general orbit $\phi(t, t_0, x_0)$ of a nonlinear non autonomous system $\dot{x} = f(x, t)$ is checked by placing a small perturbation δ at $t = t_0$ and by observing how "close" the new orbit will be regarding to $\phi(t, t_0, x_0)$. In order to do that, we quantify the difference $\phi(t, t_0, x_0 + \delta) - \phi(t, t_0, x_0)$ which can be expressed by using a Taylor series expansion on the perturbed orbit, as follows:

$$\phi(t, t_0, x_0 + \delta) - \phi(t, t_0, x_0) = \frac{\partial \phi(t, t_0, x_0)}{\partial x_0}\delta.$$

Hence, the crucial quantity that will allow us to determine the effect of the perturbation is the square matrix $\Phi(t, t_0, x_0) = \partial\phi(t, t_0, x_0)/\partial x_0$ which is the state transition matrix and effectively describes how the perturbations will evolve with respect to time. For linear time invariant systems ($\dot{x}(t) = Ax(t) + B$), $\Phi(t, t_0, x_0) = e^{A(t-t_0)}$, while if the system is linear non-autonomous ($\dot{x}(t) = A(t)x(t) + B(t)$), then this matrix can be found numerically [40] by solving the following initial value problem:

$$\frac{d\Phi(t, t_0, x_0)}{dt} = A(t)\Phi(t, t_0, x_0), \qquad \Phi(t_0, t_0, x_0) = I.$$

If the vector field is nonlinear then using the fundamental theorem of calculus we have

$$\phi(t, t_0, x_0) = x_0 + \int_0^t f(\phi(s, t_0, x_0), s)ds. \tag{8}$$

Then by taking the partial derivative with respect to the initial condition we get to

$$\frac{\partial \phi(t, t_0, x_0)}{\partial x_0} = I + \int_0^t A(s, t_0, x_0)\frac{\partial \phi(s, t_0, x_0)}{\partial x_0}ds \tag{9}$$

with

$$A(t, t_0, x_0) = \left.\frac{\partial f(x, t)}{\partial x}\right|_{x=\phi(t,t_0,x_0)}. \tag{10}$$

Finally, by differentiating (9) with respect to time we get the following differential equation:

$$\frac{d}{dt}\left(\frac{\partial \phi(t, t_0, x_0)}{\partial x_0}\right) = A(t, t_0, x_0)\frac{\partial \phi(t, t_0, x_0)}{\partial x_0} \tag{11}$$

which can be solved numerically. In the case where the orbit under study is periodic (like in a DC-DC converter), the state transition matrix evaluated at $t = t_0 + T$ is called the monodromy matrix with the following property:

$$\Phi(nT + t_0, t_0, x_0) = [\Phi(T + t_0, t_0, x_0)]^n.$$

Hence, using eigendecomposition of the monodromy matrix we can state that if all the eigenvalues of the monodromy matrix have magnitude less than 1 then the perturbations $\phi(t, t_0, x_0 + \delta) - \phi(t, t_0, x_0)$ will converge to zero and therefore the periodic orbit under study is stable. The expression of the monodromy matrix obtained by this procedure coincides with the Jacobian matrix of the iterated mapping.

B. Nonsmooth Orbits

When the periodic orbit crosses the switching manifolds the vector field becomes nonsmooth and therefore we cannot use the aforementioned approach to determine its stability. In order to better understand that, let's assume that we have the nonsmooth orbit shown in Fig. 3[3] with t_0 the point where a perturbation is placed, t_s is the instant when the orbit under study hits the switching manifold and $\bar{t}_s$ when the perturbed orbit crosses the manifold. As, $t_s \neq \bar{t}_s$ there is a problem in describing the perturbation vectors during the interval $[t_s, \bar{t}_s]$. Filippov [38] suggested a matrix called *Saltation matrix* or *jump matrix* that maps

[3]The perturbation is intentionally displayed so large in order to improve the quality of the figure.

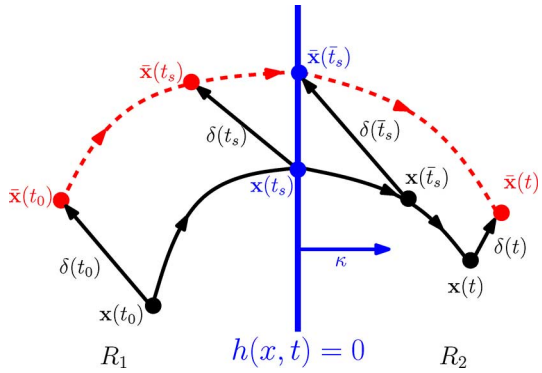

Fig. 3. The original orbit x and the perturbed orbit $\overline{x}$ close to the switching point. To improve the visibility the perturbation vectors $\phi(t_k, t_0, x_0 + \delta) - \phi(t_k, t_0, x_0)$ are written as $\delta(t_k)$.

the perturbation vector $\delta(t_s)$ to $\delta(\bar{t}_s)$ These two vectors are defined as follows:

$$\delta(t_s) = \overline{x}(t_s) - x(t_s) \quad \text{and} \quad \delta(\bar{t}_s) = \overline{x}(\bar{t}_s) - x(\bar{t}_s)\,. \tag{12}$$

Using a Taylor series expansion in the perturbed and initial orbits with respect to t at $t = t_s$ it can be found that

$$x(\bar{t}_s) = x(t_s) + f_2(x(t_s), t_s) \cdot \delta t \tag{13}$$
$$\overline{x}(\bar{t}_s) = \overline{x}(t_s) + f_1(\overline{x}(t_s), t_s) \cdot \delta t \tag{14}$$

were $\delta t = \bar{t}_s - t_s$. By combining (13), and (14) we have

$$\delta(\bar{t}_s) = \overline{x}(t_s) - x(t_s) + (f_1(\overline{x}(t_s), t_s) - f_2 x((t_s), t_s)) \cdot \delta t \tag{15}$$

which implies that

$$\delta(\bar{t}_s) = \delta(t_s) + (f_1(\overline{x}(t_s), t_s) - f_2(x(t_s), t_s)) \cdot \delta t. \tag{16}$$

Also using (13) and (14), one gets

$$\overline{x}(\bar{t}_s) = x(t_s) + \delta(t_s) + f_1(\overline{x}(t_s), t) \cdot \delta t. \tag{17}$$

Now, using a Taylor series expansion on $h(x(t), t)$ at $(x(t_s), t_s)$ and by denoting as $h_x(x_s, t_s) = \kappa^\intercal$, i.e., the gradient of the function $h(x(t), t)$ or equivalently the vector normal to the switching manifolds and taking into account that $h(x(t_s), t_s) = 0$ we have

$$h(x(t), t) = \kappa^\intercal \cdot (x(t) - x(t_s)) + h_t(x_s, t_s) \cdot (t - t_s). \tag{18}$$

By evaluating this expression at $\left(\overline{x}(\bar{t}_s), \bar{t}_s\right)$ we have $h(\overline{x}(\bar{t}_s), \bar{t}_s) = 0$ which implies that

$$\kappa^\intercal \cdot (\overline{x}(\bar{t}_s) - x(t_s)) + h_t(x_s, t_s) \cdot \delta t = 0. \tag{19}$$

Using (17) in (14) we have

$$\kappa^\intercal \cdot \left(\delta(t_s) + f_1(\overline{x}(t), t) \cdot \delta t\right) + h_t(x_s, t_s) \cdot \delta t = 0. \tag{20}$$

This defines the time required between the $\bar{t}_s$ and t_s

$$\delta t = \frac{-\kappa^\intercal \cdot \delta(t_s)}{\kappa^\intercal \cdot f_1(\overline{x}(t), t) + h_t(x_s, t_s)}. \tag{21}$$

By inserting (21) into (16) we have

$$\delta(\bar{t}_s) = \left(I + \frac{(f_2(x(t_s), t_s) - f_1(\overline{x}(t_s), t_s)) \cdot \kappa^\intercal}{\kappa^\intercal \cdot f_1(\overline{x}(t), t) + h_t(x_s, t_s)}\right) \delta(t_s). \tag{22}$$

Note that if the trajectory encounters the switching surface tangentially then the term $\kappa^\intercal f_1$ in the denominator of (21) will be zero. Consequently, if the switching function is time invariant then the trajectory must encounter the switching surface transversally, otherwise δt will be infinitely large. Finally, as at t_s we have that $\overline{x}(t_s) = x(t_s)$ (i.e., there are no jumps in the state space)

$$S = I + \frac{(f_2(x(t_s), t_s) - f_1(x(t_s), t_s)) \cdot \kappa^\intercal}{\kappa^\intercal \cdot f_1(x(t), t) + h_t(x_s, t_s)}. \tag{23}$$

The matrix S in (23) is the Saltation matrix and in the next section will be used in order to determine the stability of the desired periodic orbit of a DC-DC converter.

C. Stability Analysis of Nonsmooth Periodic Orbits

Now it is possible to calculate the monodromy matrix of a nonsmooth dynamical system such as a DC-DC converter[4]. Assume that we have an orbit in the state space with one switching manifold Σ that splits the state space into two compartments R_1 and R_2. The orbit starts at $t = t_0$ in R_1, and then it hits the switching manifold Σ when $t = t_1$, at $t = t_2$ it hits Σ again and returns to the original point after $T - t_2$ seconds. In this case from t_0 until t_1 we have a smooth orbit and the perturbation vectors can be described by a state transition matrix $\Phi_1(t_1, t_0, x_0)$; similarly for the intervals $[t_1,\ t_2]$ and $[t_2,\ t_0 + T]$ with $\Phi_2(t_2, t_1, x(t_1))$ and $\Phi_3(t_0 + T, t_2, x(t_2))$ respectively. If the vector fields in (1) are linear then these state transition matrices can easily be computed using the exponential matrix, while if they are nonlinear then (11) will have to be solved numerically. Finally, the perturbation vectors near the switching points can be represented by two Saltation matrices S_1 and S_2 and therefore the overall monodromy matrix $\Phi(t_0 + T, t_0, x_0) := M$ is

$$M = \Phi_3(t_0 + T, t_2, x(t_2)) \cdot S_2 \cdot \Phi_2(t_2, t_1, x(t_1)) \cdot S_1 \cdot \Phi_1(t_1, t_0, x_0). \tag{24}$$

This matrix coincides with the Jacobian of the iterated map and can be used for accurate stability analysis of the converter.

D. Use of the Saltation Matrix to Avoid Instabilities

Once the monodromy matrix is derived it is possible to be used not only for the stability analysis but also to ensure a stable response. One way to do that is to calculate for a range of parameter variables (e.g., the supply voltage, output load, inductance and capacitance) all the Floquet multipliers and choose the proper values of the parameters that offer a stable response. While this may be possible in some cases, it cannot be generalized. For example, the supply voltage of a power converter

[4]As it has been briefly previously stated, in electrical systems we do not have jumps in the state space and therefore the generic nonsmooth limit cycle will be nonsmooth but continuous. In the case where a jump takes place in the state space then probably the most suitable methods of analysis are the Discontinuity Map [28] and trajectory sensitivities [50].

that is fed by a PV greatly changes from full power during the day to zero during the night, similarly the load may considerably fluctuate. Furthermore, the inductance and capacitance are usually designed based on the desired current/voltage ripple and hence they cannot be altered. The control structure is also designed based on the requirements for transient response and steady-state error. Therefore, it is highly possible to be in a case where the stable operating region is very limited or as it is most commonly the case, the designer to have to use larger values for the inductance and capacitance with a direct result on the size and cost of the converter. This problem is conventionally addressed in current mode control by using a ramp compensator, but this approach introduces a steady state error and more importantly it slows down the system's response [59]. In [42] the structure of the Saltation matrix was used to address this problem without making any invasive changes to either the converter or the controller. Looking again at the expression of (22), we see that the Saltation matrix and hence the Floquet multipliers depend on the vector fields before and after the switching (i.e., the converter/controller structure and parameters) and on the switching manifold. A key observation is the dependence on the switching manifold is on its partial derivative with respect to the states and time. Therefore in [42] it was suggested to inject a small amplitude-high frequency signal in the controller that will have negligible effect on the slow scale dynamics of the converter but due to the partial derivative with respect to time will have a major effect on the Floquet multipliers. Therefore it is possible to widen the stability region.

V. Trajectory Sensitivity

Trajectory sensitivities describe the change in a trajectory resulting from perturbations in initial conditions[5]. Consider a nonlinear, non-autonomous system of the form

$$\dot{x} = f(x, t, \rho), \quad x(t_0) = x_0. \tag{25}$$

Dynamic behavior can be expressed analytically by the *flow*

$$x(t) = \phi(t, t_0, x_0). \tag{26}$$

A Taylor series expansion of (26) gives

$$\delta x(t) = \phi(t, t_0, x_0 + \delta x_0) - \phi(t, t_0, x_0) \approx \frac{\partial \phi(t, t_0, x_0)}{\partial x_0} \delta x_0 \tag{27}$$

where $\Phi(t, t_0, x_0) \triangleq \partial \phi(t, t_0, x_0)/\partial x_0$ is referred to as the *sensitivity transition matrix* or simply *trajectory sensitivities*. As previously discussed, trajectory sensitivities evolve along smooth sections of an orbit according to the variational equations

$$\frac{d}{dt}\Phi(t, t_0, x_0) = \left.\frac{\partial f(x,t)}{\partial x}\right|_{x=\phi(t,t_0,x_0)} \Phi(t, t_0, x_0)$$
$$\Phi(t_0, t_0, x_0) = I \tag{28}$$

where I is the appropriately sized identity matrix. When a switching condition $h(x, t) = 0$ is encountered, the trajectory sensitivities undergo a jump according to (22). These concepts are extended to hybrid dynamical systems in [50], where the model has a differential-algebraic structure, allows arbitrarily complicated switching conditions and incorporates state reset (jump) actions. Trajectory sensitivities can be computed efficiently if an implicit numerical integration technique, such as trapezoidal integration, is used to establish the nominal trajectory. Such techniques invoke Newton's method at each step along the integration path therefore require Jacobian information. Trajectory sensitivities can be obtained as a by-product of that solution process. Full details are provided in [50]. Points x_0 on the orbit of a nonautonomous limit cycle with period T satisfy

$$x(t_0 + T) = \phi(t_0 + T, t_0, x_0) = x_0. \tag{29}$$

Computing this orbit yields, for very little extra computational cost, the trajectory sensitivities $\Phi(t_0 + T, t_0, x_0)$. But note that this is exactly the monodromy matrix M. Consequently, stability information can be obtained as a by-product of simulation, with switched systems introducing no extra complications.

The availability of trajectory sensitivities makes locating limit cycles a straightforward process. Rearranging (29) gives

$$F(x) = \phi(t_0 + T, t_0, x) - x = 0 \tag{30}$$

which can be solved using Newton's method

$$x^{k+1} = x^k - [DF(x^k)]^{-1} F(x^k) \tag{31}$$

where k denotes the iteration number, and

$$DF(x^k) = \Phi(t_0 + T, t_0, x^k) - I.$$

Evaluating $F(x^k)$ involves numerical integration to obtain the flow $\phi(t_0+T, t_0, x^k)$. The sensitivities $\Phi(t_0+T, t_0, x^k)$ that are required for DF are available from the computation of the flow. Solution processes such as (31) that require simulation as part of Newton's method are referred to as shooting methods [57]. Even though most power converters employ an external clock, there are some topologies (like when a hysteresis controller is used) that result in autonomous systems [58]. In this case these ideas can naturally extend to autonomous systems [62]. The extension to continuation processes, for producing bifurcation diagrams, is also straightforward [62]. Limit cycles associated with border collisions can be obtained by augmenting (30) with equations that describe a tangential encounter between the orbit and a switching surface [62].

VI. Steady-State Analysis

Although the methods presented previously can be used to obtain numerically the critical value of the parameters at the onset of instability, it would be more useful to have explicit expressions for the stability boundaries. For instance, in many applications, the feedback coefficients, poles and zeroes of the controllers are design parameters that should be adjusted accordingly to the power stage to be controlled. Our purpose in this section is to present analytical expressions at the onset of SN and PD singularities. Unfortunately, this is not a universal procedure to obtain the boundary curves but it will always work

[5]Sensitivity to perturbations in parameters ρ can also be captured by modelling parameters as "states" through the introduction of trivial differential equations $\dot{\rho} = 0$.

for systems switching between two configurations. More specifically, let us consider a power converter that can be modeled by the following piecewise linear state equation:

$$\dot{x} = \begin{cases} A_1 x + B_1 w, & \text{if } 0 \le t < d_n T \\ A_2 x + B_2 w, & \text{if } d_n T \le t < T \end{cases} \tag{32}$$

which can be conveniently written in the following form:

$$\dot{x} = (A_1 x + B_1 w)u + (A_2 x + B_2)(1-u). \tag{33}$$

Note that in the special case where $A_1 = A_2$, the converter power stage is linear and therefore a linear transfer function describes the relationship between the driving signal u and the control signal v_c. In such cases, in [52] a Fourier series expansion was applied to derive closed form expressions for the stability boundaries. However in the general case $A_2 \neq A_1$ which will result in a *bilinear* model as it can be observed from (33). In such cases a different approach can be taken. The key point here is that independently on whether $A_2 = A_1$ or not, for each switching subinterval, the system equations (for most switching converters) are linear and time-invariant and hence closed form solutions can be found (3). For convenience of notation, let us express the switching condition as $h(t) = \kappa^{\intercal}(X_r(t) - x(t)) - v_{\text{ramp}}(t) = 0$ which results from the comparison of the ramp signal and the control signal, with X_r being a suitable reference vector, κ the feedback gain which is also the gradient of the switching function h and $x \in \mathbb{R}^m$ is the vector of the state variables including the power stage and the controller. Note that the switching condition can also be written as $h(t) = -\kappa^{\intercal}x(t) - r(t) = 0$, where $r(t) = v_{\text{ramp}}(t) - \kappa^{\intercal}X_r(t)$. As a case study, let us focus on converters under Trailing Edge Modulation (TEM) strategies during steady-state in which D is the steady-state duty cycle and the state of the switch is ON for $t \in [0, DT]$[6]. According to (3) we have that $\Phi_1(DT) = e^{A_1 DT}$ and $\Phi_2(DT) = e^{A_2(1-D)T}$, $\Psi_1(DT) = \int_0^{DT} e^{A_1 s} B_1 w ds$ and $\Psi_2(DT) = \int_0^{(1-D)T} e^{A_2 s} B_2 w ds$. Let us also denote with x_{ss} the state vector when the steady-state is reached, i.e., $x_{\text{ss}}(0)$ is the state vector at the beginning of the clock period and $\mathbf{x}_{\text{ss}}(DT)$ the state vector at $t = DT$.

During steady-state operation, at $t = 0$ the switch is set to ON and the converter is being described by f_1 [see (1)] while it becomes OFF when $-\kappa^{\intercal}x(DT) - r(DT) = 0$ (Fig. 4) with f_2 being the vector field during $t \in [DT,\ T]$. By enforcing T–periodicity and evaluating the resulting expressions at $t = DT$ and $t = T$ (or $t = 0$) we obtain

$$x_{\text{ss}}(DT) = (I - \Phi(DT))^{-1}\Psi(DT) \tag{34}$$

$$x_{\text{ss}}(0) = (I - \overline{\Phi}(DT))^{-1}\overline{\Psi}(DT) \tag{35}$$

where

$$\begin{aligned} \Phi(DT) &= \Phi_1(DT)\Phi_2(DT) \\ \Psi(DT) &= \Phi_1(DT)\Psi_2(DT) + \Psi_1(DT) \\ \overline{\Phi}(0) &= \Phi_2(0)\Phi_1(0) \\ \overline{\Psi}(0) &= \Phi_2(0)\Psi_1(0) + \Psi_2(0). \end{aligned}$$

[6]The results can easily be adapted for Leading Edge Modulation (LEM) strategies by just replacing D with $1 - D$ and a simple sign inversion in the feedback coefficients.

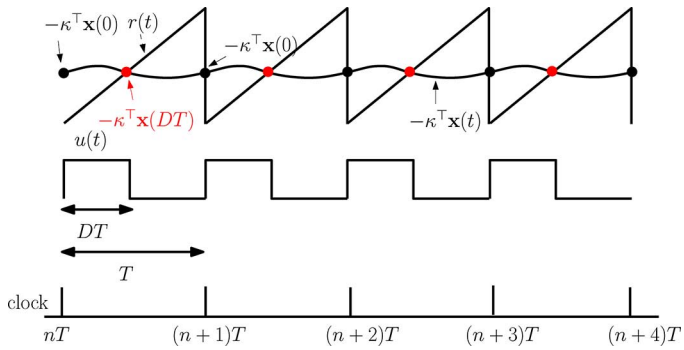

Fig. 4. Waveforms of the T–periodic external signal $r(t)$ and the feedback signal $\kappa^{\intercal}x_{\text{ss}}(t)$ at T–periodic regime.

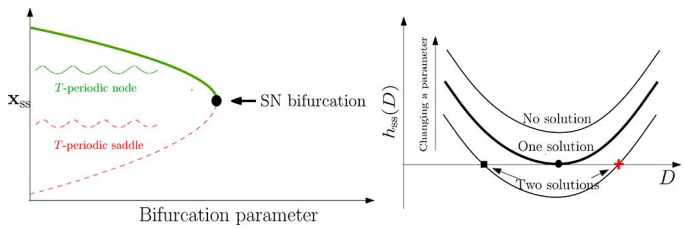

Fig. 5. SN bifurcation scenario in a switching converter.

Obviously for (34) and (35) to hold the matrices $I - \Phi$ and $I - \overline{\Phi}$ must be non-singular and two kinds of singularities may appear here due to the structure of the matrices A_i and Φ. The first one is a nonstructural singularity and can be avoided by just adding parasitic resistances in the state matrix. The second one is a structural singularity due to the presence of an integrator in the feedback loop that adds a pole in the origin. In that case the expression in (34) excludes the state variable corresponding to the integral action. Finally, it is possible to express the switching manifold h using (34) as

$$h_{\text{ss}}(DT) := -\kappa^{\intercal}(I - \Phi(DT))^{-1}\Psi(DT) - r(DT) = 0. \tag{36}$$

A. SN Bifurcation Boundary

Using (36) it is possible to determine the onset of a Saddle-Node bifurcation. To do that, notice that the number of solutions of (36) equals to the number of period 1 orbits that exist for a specific set of parameters. One way to locate the bifurcation point is to numerically solve (36), find the duty cycles for each point and then use (35) to locate the fixed points. When two fixed points coincide then we have SN bifurcation. Unfortunately this is not a simple task as the numerical solution may be inaccurate, the expression for (36) may be very complicated and also we need to use several initial conditions to make sure that we locate all the fixed points. An alternative is to notice that at a SN bifurcation boundary there is a tangency between $h_{\text{ss}}(D)$ and the D-axis in such a way that two solutions of (36) coalesce and disappear (Fig. 5)

$$\frac{\partial h_{\text{ss}}(D)}{\partial D} = 0 \Rightarrow -\frac{\partial \kappa^{\intercal}x_{\text{ss}}(DT)}{\partial D} = \frac{\partial r(DT)}{\partial D}. \tag{37}$$

Let m_a be the slope of the external T–periodic signal $r(t)$. Therefore (37) becomes

$$-\kappa^{\intercal}\frac{\partial x_{\rm ss}(DT)}{\partial D} - m_a T = 0. \tag{38}$$

By calculating the partial derivative in (38) using the expression of $x_{\rm ss}(DT)$ in (34), the expression of the critical slope of the ramp signal at a SN bifurcation boundary is as follows:

$$m_{a,\rm SN}(D) = -\kappa^{\intercal}(I-\Phi)^{-1}\Phi_1(f_1(x_{\rm ss}(0)) - f_2(x_{\rm ss}(0)))). \tag{39}$$

More calculation details can be found in [54]. It has to be mentioned here that in [52], the same condition has been derived, but expressed in a different form, imposing an eigenvalue equal to +1 in the characteristic equation of the Jacobian matrix.

B. Steady-State Response to Subharmonic Excitation

In switching converters with two configurations, during the switching cycle of duration T, the system has two phases defined by the system matrices (A_1, B_1) and (A_2, B_2) respectively. During the switching cycle of duration $2T$, the system has four phases defined by the system matrices (A_1, B_1), (A_2, B_2), (A_1, B_1) and (A_2, B_2) respectively. During two consecutive switching periods in the interval $(nT, (n+2)T)$, let the crossing between the signals $-\kappa x(t)$ and $r(t)$ occur at $t = (D - \varepsilon_t + n)T$ and at $t = (1 + D + \varepsilon_t + n)T$, $n \in \mathbb{Z}$ (see Fig. 6). The parameter ε_t is a small quantity that vanishes at the boundary between period 1 and period 2 behavior. At this point, the period 1 solution and the period 2 solution coincide. By obtaining the expression of the period 2 steady-state solutions at the switching instants, setting the corresponding constraints imposed by the feedback and equating these solutions at the critical point ($\varepsilon_t \to 0$), a condition for predicting PD bifurcation is obtained. Exhibiting a period 2 regime, the sampled value of the steady-state variables at the switching instants $(D - \varepsilon_t)T$ and $(D + 1 + \varepsilon_t)T$ can be obtained by using the exact solution of the trajectory in the time domain and forcing period 2 regime. In doing so, they can be expressed as follows:

$$x_{\rm ss}((D-\varepsilon_t)T) = (I - \Phi_-(\varepsilon_t))^{-1}\Psi_-(\varepsilon_t) \tag{40a}$$
$$x_{\rm ss}((D+1+\varepsilon_t)T) = (I - \Phi_+(\varepsilon_t))^{-1}\Psi_+(\varepsilon_t) \tag{40b}$$

where

$$\Phi_-(\varepsilon_t) = \overline{\Phi}_1\overline{\Phi}_4\overline{\Phi}_3\overline{\Phi}_2,\ \Phi_+(\varepsilon_t) = \overline{\Phi}_3\overline{\Phi}_2\overline{\Phi}_1\overline{\Phi}_4 \tag{41a}$$
$$\Psi_-(\varepsilon_t) = \overline{\Phi}_1\overline{\Phi}_4\overline{\Phi}_3\overline{\Psi}_2 + \overline{\Phi}_1\overline{\Phi}_4\overline{\Psi}_3 + \overline{\Phi}_1\overline{\Psi}_4 + \overline{\Psi}_1 \tag{41b}$$
$$\Psi_+(\varepsilon_t) = \overline{\Phi}_3\overline{\Phi}_2\overline{\Phi}_1\overline{\Psi}_4 + \overline{\Phi}_3\overline{\Phi}_2\overline{\Psi}_1 + \overline{\Phi}_3\overline{\Psi}_2 + \overline{\Psi}_3 \tag{41c}$$

and

$$\bar{\Phi}_1 = \Phi_1 e^{-A_1\varepsilon_t T},\ \bar{\Psi}_1 = \int_0^{(D-\varepsilon_t)T} e^{A_1\tau}{\rm d}\tau B_1 u \tag{42a}$$
$$\bar{\Phi}_2 = \Phi_2 e^{A_2\varepsilon_t T},\ \bar{\Psi}_2 = \int_0^{(1-D+\varepsilon_t)T} e^{A_2\tau}{\rm d}\tau B_2 u \tag{42b}$$
$$\bar{\Phi}_3 = \Phi_1 e^{A_1\varepsilon_t T},\ \bar{\Psi}_3 = \int_0^{(D+\varepsilon_t)T} e^{A_1\tau}{\rm d}\tau B_1 u \tag{42c}$$
$$\bar{\Phi}_4 = \Phi_2 e^{-A_2\varepsilon_t T},\ \bar{\Psi}_4 = \int_0^{(1-D-\varepsilon_t)T} e^{A_2\tau}{\rm d}\tau B_2 u. \tag{42d}$$

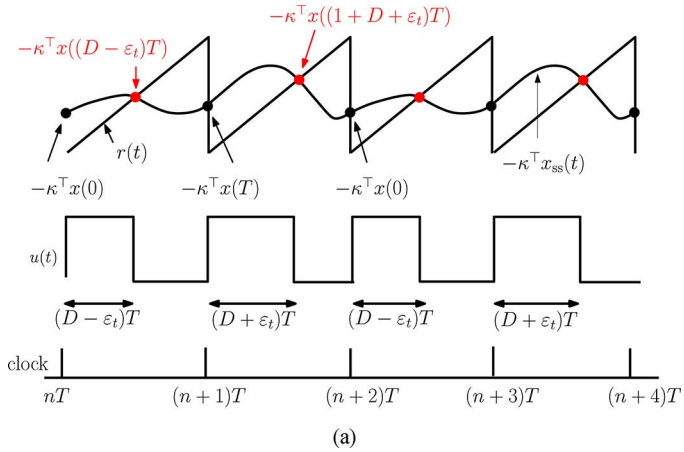

(a)

Fig. 6. Waveforms before and after the bifurcation takes place by sweeping a parameter. Waveforms of the periodic external signal $r(t)$ and the control signal $\kappa^{\intercal}x_{\rm ss}(t)$ at $2T$-periodic regime.

C. PD Bifurcation Boundary

From the switching conditions imposed by the PWM process at time instants $(D - \varepsilon_t)T$ and $(D + 1 + \varepsilon_t)T$, the following equalities hold (see Fig. 6):

$$-\kappa^{\intercal}x_{\rm ss}((D-\varepsilon_t)T) = r((D-\varepsilon_t)T) \tag{43a}$$
$$-\kappa^{\intercal}x((D+1+\varepsilon_t)T) = r((D+\varepsilon_t)T). \tag{43b}$$

Subtracting (43a) from (43b) and taking the limit when $\varepsilon_t \to 0$, using (40a) and (40b), the following expression for the critical slope at a PD bifurcation boundary is obtained:

$$m_{a,\rm PD}(D) = -\kappa^{\intercal}(I+\Phi)^{-1}\Phi_1(f_1(x_{\rm ss}(0)) + f_2(x(0))). \tag{44}$$

More calculation details can be found in [54]. It is worth mentioning here that in [52], a slightly differently expressed condition has been obtained using a different approach based on solving the eigenvalue problem of the characteristic equation or equivalently the time-domain Jacobian matrix, for the same boundary condition. Although they are expressed differently, the critical ramp slope for PD bifurcation given in (44) and the one derived in [52] coincide.

VII. Practical Examples

A. Stability Analysis Using Floquet Theory Combined by Filippov Method and the Saltation Matrix

In the previous sections we have seen the definition of stability applied in a general orbit, how this is materialized in a closed orbit and finally how to use the Saltation matrix in order to map the perturbation vectors from just before to just after a switching takes place in the state space. We have also seen how the state transition matrices combined with Saltation matrices can create the overall monodromy matrix.

1) Example 1: Now, we will apply this method to a classical example of voltage controlled buck converter, as first reported in [26][7]. The material in this subsection is mainly taken from

[7]The parameters according to [26] are: $v_{\rm in} = 24$ V, $V_{\rm ref} = 11.3$ V, $L = 20$ mH, R $= 22\ \Omega$, $C = 47\ \mu$F, $a = 8.4$, $T = 400\ \mu$s, $V_L = 3.8$ V and $V_U = 8.2$ V

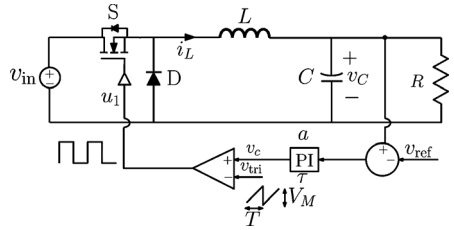

Fig. 7. Buck converter under a PI VMC scheme.

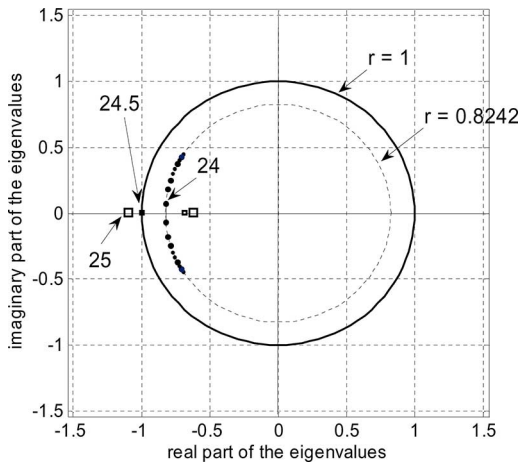

Fig. 8. Eigenvalues loci for $v_{\rm in} \in [14\ {\rm V}, 25\ {\rm V}]$. Squares indicate unstable system, solid circles stable system.

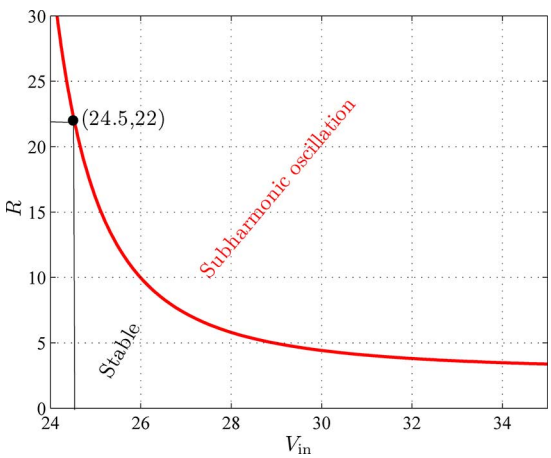

Fig. 9. Subharmonic oscillation curve in terms of the input voltage $v_{\rm in}$ and the load resistance R for a buck converter under a VMC scheme.

[42] which was the first paper in the area of power converters that utilized the concept of the Saltation matrix. The schematic circuit diagram are shown in Fig. 7. In the voltage mode controlled buck converter the error signal between the demanded voltage $V_{\rm ref}$ and the actual output voltage v is fed to a proportional controller (with gain a) and the resulted control signal v_c is compared with a ramp signal $v_{\rm ramp}$; the result of this comparison determines the state of the switch. By defining $x_1(t) = v(t)$ and $x_2(t) = i(t)$ (the inductor current), the state equations of the buck converter may be written as follows:

$$\dot{x} = \begin{cases} A_1 x + B_1 w, & a(x_1(t) - V_{\rm ref}) < v_{\rm ramp}(t) \\ A_2 x + B_2 w, & a(x_1(t) - V_{\rm ref}) > v_{\rm ramp}(t). \end{cases} \tag{45}$$

where, $w = v_{\rm in}$ and

$$A_1 = A_2 = \begin{pmatrix} -\frac{1}{RC} & \frac{1}{C} \\ -\frac{1}{L} & 0 \end{pmatrix}, \quad B_1 = \begin{pmatrix} 0 \\ \frac{1}{L} \end{pmatrix}.$$

The equation defining the switching hypersurface is given by

$$h(x(t), t) = a x_1(t) - r(t) = 0,\ a \neq 0 \tag{46}$$

$$r(t) = a V_{\rm ref} + v_{\rm ramp}(t) \tag{47}$$

where $v_{\rm ramp}(t) = V_L + (V_U - V_L)(t/T) \bmod 1$ is the modulator ramp. This will result into

$$\frac{\partial h(x(t), t)}{\partial t} := h_t(x(t), t) = -\frac{V_U - V_L}{T} = -m_a$$

where m_a is the slope of the ramp modulator. The gradient of the switching function h can be calculated as follows:

$$\kappa = h_x(x(t), t) = \nabla h(x(t), t) = \begin{pmatrix} \frac{\partial h(x(t),t)}{\partial x_1(t)} \\ \frac{\partial h(x(t),t)}{\partial x_2(t)} \end{pmatrix} = \begin{pmatrix} a \\ 0 \end{pmatrix}. \tag{48}$$

Hence the saltation matrix (23) is expressed by

$$S = \begin{pmatrix} \frac{1}{\frac{v_{\rm in}}{L}} & 0 \\ \frac{x_2(t_s) - \frac{x_1(t_s)}{R}}{C} - m_a & 1 \end{pmatrix}. \tag{49}$$

The nominal operation of the converter is an oscillatory motion around the desired value with a frequency that equals that of the external clock. Notice here that there will be 2 switching events in one clock cycle, one at $t = DT$ (where $1 - D$ is the duty cycle) and one at $t = T$ and therefore it may be wrongly assumed that we need to use the Saltation matrix twice. While this is true, at $t = T$ there is a forced commutation and therefore the nominal and the perturbed orbit will hit the switching manifold at the same instant. This implies that the Saltation matrix at $t = T$ is the identity matrix. Another way to state this, is that at $t = T$ the ramp signal is discontinuous and hence the derivative of h with respect to time is infinite resulting in the Saltation matrix being the identity matrix. Now we need the state transition matrices for the two subsystems. The state transition matrices are given by $\Phi_1(t_s, 0) = e^{AdT}$ and $\Phi_2(T, t_s) = e^{A((1-d)T)}$, as the subsystems are linear time invariant. The eigenvalues of this matrix (also called Floquet multipliers) are shown in Fig. 8 indicating that a PD bifurcation occurs at approximately 24.5 V which agrees with the numerical simulations shown in [42]. The same results can be obtained from a discrete-time map.

B. Stability Boundaries Using Steady-State Analysis

1) Example 2: Consider the same example as before with the same parameter values except the load resistance which is considered as a secondary bifurcation parameter. Fig. 9 shows the boundary in terms of the load resistance R and the input voltage $v_{\rm in}$ obtained from (44) for the system. It can be observed that when for instance $R = 22\ \Omega$, the critical value of $v_{\rm in}$ for subharmonic oscillation occurrence is very close to 24.5 V in a perfect agreement with the previous analysis based on Floquet theory and Poincaré map modelling. It should be noted that this example uses an LEM strategy and a change of variable $D \to (1 - D)$ must be done in (44) together with a sign inversion in the voltage feedback gain.

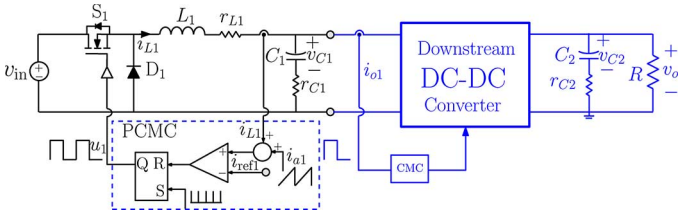

Fig. 10. Schematic circuit diagram of a buck converter under a current mode control feeding a boost converter also under current mode control.

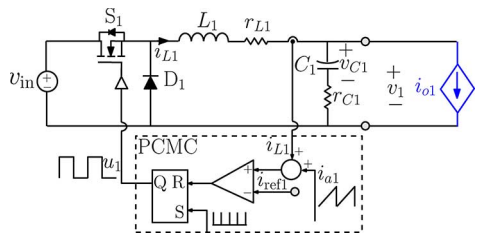

Fig. 11. Schematic circuit diagram of a buck converter under a current mode control feeding a constant current source as a load representing another converter under current mode control.

2) Example 3: In distributed DC power systems applications, often, a source converter regulated a dc bus from an energy source while at the same time loaded by a downstream converter. This kind of interconnected topologies appear in many applications such as electric vehicle, aircraft among others [9]. The system that will be considered in this example is a buck converter driving another DC-DC converter, Fig. 10. Both converters are under current mode control (CMC). The second converter can be approximated by a constant current sink as it shown in Fig. 11. Previous studies has shown that saddle-node bifurcation in this interconnected scheme results in complex interaction that cannot be predicted by averaged models [63]. It should be noted that if instead of the current, the voltage of the load converter is regulated, the output of the source converter can be approximated by a constant power sink [64], [65]. In that case the system configurations for each switch state will be nonlinear and closed form solution is not available. However, if we are concerned with the fast-scale instability analysis, current sink output approximation can still be used and the current output is given by $i_{o1} = P/v$, where P is the power and v is the output voltage. It should also be noted that the previous arguments also apply in the case if many loads are connected to the source converter and all of them can be represented by a constant power sink or constant power source as it is the case of a micro or a nano grid. The system matrices and vectors are as follows:

$$A_1 = A_2 = \begin{pmatrix} 0 & \frac{1}{C_1} \\ -\frac{1}{L_1} & -\frac{r_{L1}+r_{C1}}{L_1} \end{pmatrix}$$

$$B_1 = \begin{pmatrix} \frac{1}{C_1} & 0 \\ \frac{1}{L_1} & \frac{r_{C1}}{L_1} \end{pmatrix}, \quad B_2 = \begin{pmatrix} \frac{1}{C_1} & 0 \\ 0 & \frac{r_{C1}}{L_1} \end{pmatrix}$$

$$x = \begin{pmatrix} v_{C_1} \\ \\ i_{L1} \end{pmatrix}, \quad w = \begin{pmatrix} v_{\text{in}} \\ i_{o1} \end{pmatrix} \quad \kappa = \begin{pmatrix} k_i \\ 0 \end{pmatrix}.$$

The parameter values used are the same in [63] and are as follows: $v_g = 120$ V, $L_1 = 37.5\ \mu$H, $C_1 = 420\ \mu$F, $R = 10\ \Omega$, $r_{L1} = r_{C1} =, \Omega$, $i_o = 38$ A. The switching frequency used is $f_s = 1/T = 50$ kHz. Fig. 12 shows $h_{\text{ss}}(D)$ which gives the possible operating steady-state duty cycles for different values of i_{ref} just below and just above the critical point. This figure also shows the stability map of the system in the parameter space (D_1, m_{a1}). For $D_1 < 0.5$, the system has only one solution. For $D_1 > 0.5$, three different regions can be identified. The first one is $m_{a1} < m_{a,\text{SN}}$ where the system presents no solution. The second one is $m_{a,\text{SN}} < m_{a1} < v_{\text{in}}(2L)$ where the system presents one stable solution and one saddle. The last one where $m_{a1} > v_{\text{in}}(2L)$ and the system presents one stable solution. For this particular example it turns out that the boundary of the SN bifurcation in the parameter space (D, m_{a1}) is approximately a straight line whose slope is v_{in}/L and passing from $D = 0.5$ and its maximum value is $v_{\text{in}}/(2L)$ for $D = 1$. Therefore, by choosing $m_{a1} = v_{\text{in}}/(2L)$ will guarantee that the system to have only one solution independently on the value of the duty cycle.

VIII. Concluding Remarks and Future Challenges

A core component of distributed power generation systems is a power converter that interconnects local power sources to local loads. Therefore, the efficiency and proper operation of these converters are of paramount importance for the whole power grid. One of the main requirements in order to achieve this proper operation is to guarantee that the power converter's nominal periodic motion is stable despite any internal or external parameter changes. In this review/tutorial paper, four different methods were presented that address exactly this point, i.e., the stability of the nominal periodic orbit. The basic idea behind each of these methods is briefly described and simple case studies confirm their validity. Each method has its own advantages and shortcomings and one of the main goal of this paper was to highlight them in order for the user to choose the most appropriate one for his/her application.

The Poincaré map was presented that has the ability to predict all the nonlinear phenomena that are present in power converters but it can be cumbersome in complicated topologies. The Saltation matrix was also presented that greatly simplifies the analysis and results in the same matrix as the Jacobian of the Poincaré map. The trajectory sensitivity approach using a discrete-algebraic-differential model was also presented and finally a method based on the time-domain steady state-response of the converter was used in order to predict period doubling and saddle-node bifurcations.

While a lot of work has taken place in the area of stability analysis of power converters, there are still many challenges that need to be addressed. Apart from the purely theoretical interest that these systems impose, there are many practical problems that have to be resolved. The main issue that requires attention by the scientific community is the study of more complicated power converter topologies that are necessary in distributed power generation systems especially when the operating conditions greatly vary. For example in an isolated microgrid with RES, battery and a local load, the power converter must be able to handle multiple power sources with great variability in their outputs (e.g., the solar irradiation) and at the same time feed the local unpredictable load and/or charge the battery

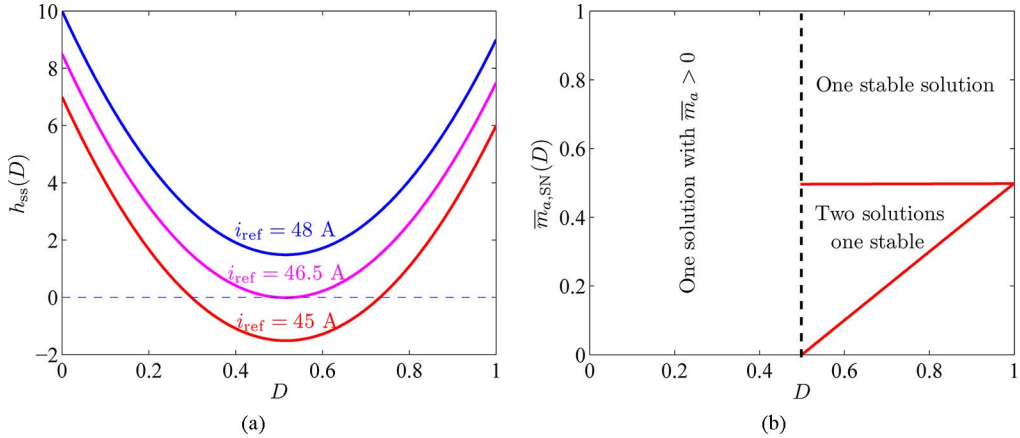

Fig. 12. Steady-state switching function h_{ss} showing the disappearance of two solutions near a SN bifurcation (a) and the stability map in terms of the duty cycle and the normalized slope $\overline{m}_a = m_a/(v_{in}/L)$ of the signal r.

(when this is required) with high efficiency and overall performance. Another interesting topic is the combination of multiple power converters in distributed power generation systems and how stability problems that appear in one converter can be isolated and not to propagate to the rest of the system. This is the case for instance of emerging fields such as in grid-to-vehicle and vehicle-to-grid interconnection using others switching converters. In these kind of interconnected schemes, the problem of accurate stability analysis using nonlinear tools tools is challenging. The analysis method can be also extended to micro and nano grids where many converters are interconnected. From a theoretical point of view a major challenge is the modifications of these methods in order to be used by power electronics practitioners for the proper design of DC-DC converters. Hence, apart from being able to predict when these instabilities will occur, the presented methodologies must be able to offer simple tools that will guarantee the stable operation of the converter and to offer easy-to-use indexes for accurately predicting the onset of instability [66], [67]. While some work has taken place on this issue (mainly on simple DC-DC converters), more work is further required.

REFERENCES

[1] B. K. Bose, "Global warming: Energy, environmental pollution, and the impact of power electronics," *IEEE Ind. Electron. Mag.*, vol. 4, no. 1, pp. 6–17, Mar. 2010.

[2] B. Fahimi, A. Kwasinski, A. Davoudi, R. S. Balog, and M. Kiani, "Powering a more electrified planet," *IEEE Power Energy Mag.*, no. 2, pp. 54–64, Aug. 2011.

[3] P. Järventausta, S. Repo, A. Rautiainen, and J. Partanen, "Smart grid power system control in distributed generation environment," *Annu. Rev. Control*, vol. 34, no. 2, pp. 277–286, Dec. 2010.

[4] S. Luo and I. Batarseh, "A review of distributed power systems Part I: DC distributed power system," *IEEE Aerospace Electron. Sys. Mag.*, vol. 20, no. 8, pp. 5–16, Aug. 2005.

[5] C. K. Tse, *Complex Behavior of Switching Power Converters*. Boca Raton, FL: CRC Press, 2003.

[6] , S. Banerjee and G. C. Verghese, Eds., *Nonlinear Phenomena in Power Electronics: Attractors, Bifurcations, Chaos, and Nonlinear Control*. New York: IEEE Press, 2001.

[7] J. G. Kassakian, M. F. Schlecht, and G. C. Verghese, *Principles of Power Electronics*. New York: Springer, 1991.

[8] R. D. Middlebrook and S. Cuk, "A general unied approach to modeling switching-converter power stages," in *Power Electron. Special.Conf.*, 1976, pp. 18–34.

[9] A. Riccobono and E. Santi, "Comprehensive review of stability criteria for DC power distribution systems," *IEEE Trans. Ind. Appl.*, vol. 50, no. 5, pp. 3525–3535, Sep./Oct. 2014.

[10] V. A. Caliskan, G. C. Verghese, and A. M. Stankovic, "Multifrequency averaging of DC/DC converters," *IEEE Trans. Power Electron.*, vol. 14, no. 1, pp. 124–133, Jan. 1999.

[11] B. Lehman and R. M. Bass, "Switching frequency dependent averaged models for PWM DC-DC converters," *IEEE Trans. Power Electron.*, vol. 11, no. 1, pp. 89–98, Jan. 1996.

[12] R. B. Ridley, "A new, continuous-time model for current-mode control," *IEEE Trans. Power Electron.*, vol. 6, no. 2., pp. 271–280, Apr. 1991.

[13] J. Sun, "Characterization and performance comparison of ripple-based control for voltage regulator modules," *IEEE Trans. Power Electron.*, vol. 21, no. 2, pp. 346–353, Feb. 2006.

[14] J. Li and F. C. Lee, "Modeling of V^2 current-mode control," *IEEE Trans. Circuits Syst. I, Reg. Papers*, vol. 57, no. 9, pp. 2552–2563, Sep. 2010.

[15] S. R. Sanders and G. C. Verghese, "Lyapunov-based control for switched power converters," *IEEE Trans. Power Electron.*, vol. 7, no. 1, pp. 17–24, Jan. 1992.

[16] C. Olalla, R. Leyva, R. A. El Aroudi, and I. Queinnec, "Robust LQR control for PWM converters: An LMI approach," *IEEE Trans. Ind. Electron.*, vol. 56, no. 7, pp. 2548–2558, Jul. 2009.

[17] C. Olalla, R. Leyva, A. El Aroudi, and P. Garcés, "QFT robust control of current-mode converters: Application to power conditioning regulators," *Int. J. Electron.*, vol. 96, pp. 503–520, 2009.

[18] C. Olalla, I. Queinnec, R. R. Leyva, and A. El Aroudi, "Optimal state-feedback control of bilinear DC–DC converters with guaranteed regions of stability," *IEEE Trans. Ind. Electron.*, vol. 59, no. 10, pp. 3868–3880, Oct. 2012.

[19] R. D. Middlebrook, "Input filter consideration in design and application of switching regulators," in *Ind. Appl. Soc. Annu. Meet.*, 1976, pp. 366–382.

[20] P. Burger, "Analysis of a class of pulse modulated DC-to-DC power converters," *IEEE Trans. Ind. Electron. Control Instrum.*, vol. 22, no. 2, pp. 104–116, May 1975.

[21] Y. A. Kuznetsov, *Elements of Applied Bifurcation Theory*. New York: Springer, 2004.

[22] R. Prajoux, J. C. Marpinard, and J. Jalade, "Etablissement de modèles mathématiques pour régulateurs de puissanceà Modulation de largeur d'impulsions (PWM). Pt. I: Modèles discrets," *ESA Sei. Tech. Rev.*, vol. 2, pp. 25–42, 1976.

[23] F. C. Lee, R. P. Iwens, Y. Yu, and J. E. Triner, "Generalized computer aided discrete-time modeling and analysis of DC–DC converters," *IEEE Trans. Ind. Electron. Control Instrum.*, vol. 26, no. 1, pp. 58–69, May 1979.

[24] G. C. Verghese, M. E. Elbuluk, and J. G. Kassakian, "A general approach to sampled-data modeling for power electronic circuits," *IEEE Trans. Power Electron.*, vol. 1, no. 2, pp. 76–89, 1986.

[25] G. C. Verghese, "Averaged and sampled-data models for current-mode control: A reexamination," in *Power Electron. Specialists Conf.*, 1989, pp. 484–491.

[26] D. C. Hamill and J. H. B. Deane, "Modeling of chaotic DC-DC converters by iterated nonlinear mappings," *IEEE Trans. Power Electron.*, vol. 7, no. 1, pp. 25–36, Jan. 1992.

[27] S. K. Mazumder, A. H. Nayfeh, and D. Boroyevich, "Theoretical and experimental investigation of the fast- and slow-scale instabilities of a DC-DC converter," *IEEE Trans. Power Electron.*, vol. 16, no. 2, pp. 201–216, Mar. 2001.
[28] M. di Bernardo, C. Budd, A. R. Champneys, and P. Kowalczyk, *Piecewise-Smooth Dynamical Systems*. London, U.K.: Springer-Verlag, 2008.
[29] M. di Bernardo and F. Vasca, "Discrete-time maps for the analysis of bifurcations and chaos in DC/DC converters," *IEEE Trans. Circuits Syst. I*, vol. 47, no. 2, pp. 130–143, Feb. 2000.
[30] M. Hagen and V. Yousefzadeh, Applying digital technology to PWM control-loop designs [Online]. Available: http://www.ti.com/download/trng/docs/seminar/
[31] D. Maksimovic and R. Zane, "Small-signal discrete-time modeling of digitally control," *IEEE Trans. Power Electron.*, vol. 22, no. 6, pp. 2552–2556, Nov. 2007.
[32] A. El Aroudi, M. Debbat, and L. Martínez-Salamero, "Poincaré maps modeling and local orbital stability analysis of discontinuous piecewise affine periodically driven systems," *Nonlinear Dynamics*, vol. 50, no. 3, pp. 431–445, Jan. 2007.
[33] C.-C. Fang and E. Abed, "Sampled-data modeling and analysis of closed-loop PWM DC-DC converters," in *Proc. 1999 IEEE Int. Symp. Circuits Syst.*, 1999.
[34] C.-C. Fang and E. H. Abed, "Sampled-data modelling and analysis of the power stage of PWM DC-DC converters," *Int. J. Electron.*, vol. 88, pp. 347–369, Mar. 2001.
[35] Y. Huang, H. H. C. Iu, and C. K. Tse, "Boundaries between fast-and slow-scale bifurcations in parallel-connected buck converters," *Int. J. Circuit Theory Appl.*, vol. 36, no. 5–6, pp. 681–695, 2007.
[36] X. Yang, H. Zhang, and X. Ma, "Modeling and stability analysis of cascade buck converters with N power stages," *Math. Comput. Simulat.*, vol. 80, no. 3, pp. 533–546, Nov. 2009.
[37] W. C. Y. Chan and K. Tse, "Study of bifurcations in current-programmed DC-DC boost converters: From quasiperiodicity to period-doubling," *IEEE Trans. Circuits Syst. I, Fundam. Theory Appl.*, vol. 44, no. 12, pp. 1129–1142, Dec. 1997.
[38] A. F. Filippov, *Differential Equations with Discontinuous Righthand Sides*. Dortrecht, The Netherlands: Kluwer, 1988.
[39] H. Dankowicz and A. B. Nordmark, "On the origin and bifurcations of stick-slip oscillations," *Physica D: Nonlinear Phenomena*, vol. 136, no. 3–4, pp. 280–302, 2000.
[40] R. I. Leine and H. Nijmeijer, *Dynamics and Bifurcations in Non-Smooth Mechanical Systems*. Berlin, Germany: Springer Verlag, 2004.
[41] H. Dankowicz and P. T. Piiroinen, "Exploiting discontinuities for stabilization of recurrent motions," *Dynamical Syst.*, vol. 17, no. 26, pp. 317–342, Dec. 2002.
[42] D. Giaouris, S. Banerjee, B. Zahawi, and V. Pickert, "Stability analysis of the continuous conduction mode buck converter via Filippov's method," *IEEE Trans. Circuits Syst. I*, vol. 55, no. 4, pp. 1084–1096, May 2008.
[43] D. Giaouris, S. Banerjee, B. Zahawi, and V. Pickert, "Control of fast scale bifurcations in power-factor correction converters," *IEEE Trans. Circuits Syst. II*, vol. 54, no. 9, pp. 805–809, Sep. 2007.
[44] D. Giaouris *et al.*, "Complex interaction between tori and onset of three-frequency quasi-periodicity in a current mode controlled boost converter," *IEEE Trans. Circuits Syst. I, Reg. Papers*, vol. 59, no. 1, pp. 207–214, Jan. 2012.
[45] D. Giaouris, S. Maity, S. Banerjee, V. Pickert, and B. Zahawi, "Application of Filippov method for the analysis of subharmonic instability in DC–DC converters," *Int. J. Circuit Theory Appl.*, vol. 37, no. 8, pp. 899–919, 2009.
[46] K. Mandal *et al.*, "An automated algorithm for stability analysis of hybrid dynamical systems," *Eur. Phys. J. Special Topics*, vol. 222, pp. 757–768, May 2013.
[47] D. Giaouris *et al.*, "Foldings and grazings of tori in current controlled interleaved boost converters," *Int. J. Circuit Theory Appl.*, vol. 42, no. 10, pp. 1080–1091, 2014.
[48] K. Mandal, S. Banerjee, and C. Chakraborty, "Symmetry-breaking bifurcation in series-parallel load resonant DC-DC converters," *IEEE Trans. Circuits Syst. I, Reg. Papers*, vol. 60, no. 3, pp. 778–787, Mar. 2013.
[49] C. Yfoulis *et al.*, "Robust constrained stabilization of boost DC-DC converters through bifurcation analysis," *Control Eng. Practice*, vol. 35, no. 0, pp. 67–82, 2015.
[50] I. A. Hiskens and M. A. Pai, "Trajectory sensitivity analysis of hybrid systems," *IEEE Trans. Circuits Syst. I, Fundam. Theory Appl.*, vol. 47, no. 2, pp. 204–220, Feb. 2000.
[51] C.-C. Fang, "Sampled-data analysis and control of DC-DC switching converters," Ph.D. dissertation, Dept. Elect. Eng., Univ. Maryland, College Park, 1997.
[52] C.-C. Fang, "Critical conditions for a class of switched linear systems based on harmonic balance: Applications to DC-DC converters," *Nonlinear Dynamics*, vol. 70, no. 3, pp. 1767–1789, 2012.
[53] A. El Aroudi, "Prediction of subharmonic oscillation in switching converters under different control strategies," *IEEE Trans. Circuits Syst. II, Exp. Briefs*, vol. 62, no. 11, pp. 910–914, Nov. 2014.
[54] A. El Aroudi, "A time-domain asymptotic approach to predict saddle-node and period doubling bifurcations in pulse width modulated piecewise linear systems, the," presented at the Int. Conf. Structural Nonlinear Dynam. Diagnosis, Agadir, Morocco, 2014.
[55] Z. T. Zhusubaliyev and E. Mosekilde, *Bifurcations and Chaos in Piecewise-Smooth Dynamical Systems*. Singapour: World Scientific, 2003.
[56] O. Dranga, B. Buti, I. Nagy, and H. Funato, "Stability analysis of nonlinear power electronic systems utilizing periodicity and introducing auxiliary state vector," *IEEE Trans. Circuits Syst. I*, vol. 52, no. 1, pp. 168–178, Jan. 2005.
[57] J. Stoer and R. Bulirsch, *Introduction to Numerical Analysis*, 2nd ed. New York: Springer, 1993.
[58] A. El Aroudi *et al.*, "Bifurcations in DC-DC switching converters: Review of methods and applications," *Int. J. Bifurcation Chaos*, vol. 15, no. 5, pp. 1549–1578, 2005.
[59] C. K. Tse and M. Lai, "Controlling bifurcations in power electronics. A conventional approach re-visited," *Latin Am. Appl. Res.*, vol. 31, pp. 177–184, 2001.
[60] I. A. Hiskens and M. A. Pai, "Trajectory sensitivity analysis of hybrid systems," *IEEE Trans. Circuits Syst. I*, vol. 47, no. 2, pp. 204–220, Feb. 2000.
[61] B. Buti, O. Dranga, H. Funato, and I. Nagy, "Stability analysis of nonlinear power electronic systems utilizing periodicity and introducing auxiliary state vector," *IEEE Trans. Circuits Syst. I, Reg. Papers*, vol. 52, no. 1, pp. 168–178, Jan. 2005.
[62] V. Donde and I. A. Hiskens, "Shooting methods for locating grazing phenomena in hybrid systems," *Int. J. Bifurcat. Chaos*, vol. 16, no. 3, pp. 671–692, Mar. 2006.
[63] A. El Aroudi *et al.*, "Bifurcation behavior in switching converters driving other downstream converters in DC distributed power systems applications, MEDYNA 2013," presented at the 1st Euro-Mediterranean Conf. Structural Dynamics Vibroacoust., Marrakech, Morocco, Apr. 2013.
[64] A. Kwasinski and C. N. Onwuchekwa, "Dynamic behavior and stabilization of DC microgrids with instantaneous constant-power loads," *IEEE Trans. Power Electron.*, vol. 26, no. 3, p. 822,834, Mar. 2011.
[65] E. Lenz and D. J. Pagano, "Nonlinear control for bidirectional power converter in a DC microgrid," presented at the 9th IFAC Symp. on Nonlinear Control Systems, Toulouse, France, Sep. 4–6, 2013.
[66] A. El Aroudi, E. Rodriguez, R. Leyva, and E. Alarcon, "A design-oriented combined approach for bifurcation prediction in switched-mode power converters," *IEEE Trans. Circuits Syst. II, Exp. Briefs*, vol. 57, no. 3, pp. 218–222, Mar. 2010.
[67] E. Rodriguez, F. Guinjoan, A. El Aroudi, and E. Alarcon, "A ripple-based design-oriented approach for predicting fast-scale instability in DC-DC switching power supplies," *Trans. Circuits Syst. I, Fundam. Theory Appl.*, vol. 59, no. 1, pp. 215–227, 2012.

Abdelali El Aroudi (M'00–SM'13) received the graduate degree in physical science from Faculté des sciences, Université Abdelmalek Essaadi, Tetouan, Morocco, in 1995, and the Ph.D. degree (hons) from Universitat Polit'ecnica de Catalunya, Barcelona, Spain, in 2000.

During the period 1999–2001 he was a Visiting Professor at the Department of Electronics, Electrical Engineering and Automatic Control, Technical School of Universitat Rovira i Virgili (URV), Tarragona, Spain, where he became an Associate Professor in 2001 and a full-time tenure Associate Professor in 2005. From September 2007 to January 2008 he was holding a visiting scholarship at the Department of Mathematics and Statistics, Universidad Nacional de Colombia, Manizales, conducting research on modeling of power electronics circuits for energy management. From February 2008 to July 2008, he was a visiting scholar at the Centre de Recherche en Sciences et Technologies de Communications et de l'Informations (CReSTIC), Reims, France. From September 2014 to December 2014, he was a visiting scholar at Institut

National des Sciences Appliquées (INSA), Université of Toulouse, France and the Laboratoire d'Analyse et d'Architecture des Systèmes (LAAS) of the Centre National de la Recherche Scientifique (CNRS), Toulouse, France. From January 2015 to July 2015, he was a visiting professor at The Petroleum Institute, Abu Dhabi, UAE. His research interests are in the field of structure and control of power conditioning systems for autonomous systems, power factor correction, stability problems, nonlinear phenomena, chaotic dynamics, bifurcations and control.

Dr. El Aroudi is a Guest Editor of the IEEE *Journal on Emerging and Selected Topics in Circuits and Systems* Special Issue on Design of Energy-Efficient Distributed Power Generation Systems (September 2015). He currently serves as Associate Editor in *IEE IET Power Electronics.*

Damian Giaouris (M'01) was born in Munich, Germany, in 1976. He received the Diploma of Automation Engineering, in 2000, from the Technological Educational Institute of Thessaloniki, Greece, the M.Sc. degree in automation and control, in 2001, and the Ph.D. degree in the area of control and stability of induction machine drives, in 2004, from Newcastle University, U.K., the B.Sc. degree in mathematics in 2009 and the Postgraduate Certificate in mathematics, in 2011, from the Open University, U.K.

He was a Lecturer in Control Systems at Newcastle University, U.K., since 2004, before moving to the Centre for Research and Technology Hellas, Greece, at the Chemical Process Engineering and Energy Resources Institute—The Laboratory of Process Systems Design and Implementation, in 2011. His research interests include nonlinear dynamics of electrical systems, distributed energy systems, smart grids, electric vehicles, and energy management.

He is a Guest Editor of the IEEE *Journal on Emerging and Selected Topics in Circuits and Systems* Special Issue on Design of Energy-Efficient Distributed Power Generation Systems, September 2015. He currently serves as Associate Editor in *IEE IET Power Electronics.*

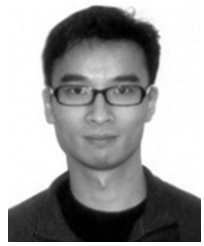

Herbert Ho-Ching Iu (S'98–M'00–SM'06) received the B.Eng. (Hons) degree in electrical and electronic engineering from the University of Hong Kong, Hong Kong, in 1997, and the Ph.D. degree from the Hong Kong Polytechnic University, Hong Kong, in 2000.

In 2002, he joined the School of Electrical, Electronic and Computer Engineering, The University of Western Australia as a Lecturer. He is currently a Professor at the same school. His research interests include power electronics, renewable energy, nonlinear dynamics, current sensing techniques, and memristive systems. He has published over 100 papers in these areas. He currently serves as an Associate Editor for *International Journal of Bifurcation and Chaos*, *IET Power Electronics* and *International Journal of Electronics*, an Editorial Board Member for *International Journal of Circuit Theory and Applications*. He is a co-editor of Control of Chaos in Nonlinear Circuits and Systems (Singapore: World Scientific, 2009) and a co-author of Development of Memristor Based Circuits (Singapore: World Scientific, 2013).

Dr. Iu has won two IET Premium Awards in 2012 and 2014. In 2014, he also won the Vice-Chancellor's Mid-Career Research Award. He currently serves as an Associate Editor for IEEE CIRCUITS AND SYSTEMS SOCIETY NEWSLETTERS. He is a Guest Editor of the IEEE *Journal on Emerging and Selected Topics in Circuits and Systems* Special Issue on Design of Energy-Efficient Distributed Power Generation Systems (September 2015).

Ian A. Hiskens (S'77–M'80–SM'96–F'06) received the B.Eng. degree in electrical engineering and the B.App.Sc. degree in mathematics from the Capricornia Institute of Advanced Education, Rockhampton, Australia, in 1980 and 1983 respectively, and the Ph.D. degree in electrical engineering from the University of Newcastle, Australia, in 1991.

He is the Vennema Professor of Engineering in the Department of Electrical Engineering and Computer Science, University of Michigan, Ann Arbor, MI, USA. He has held prior appointments in the Queensland electricity supply industry, and various universities in Australia and the United States. His research interests lie at the intersection of power system analysis and systems theory, with recent activity focused largely on integration of renewable generation and controllable loads.

Dr. Hiskens is actively involved in various IEEE societies, and is VP-Finance of the IEEE Systems Council. He is a Fellow of Engineers Australia, and a Chartered Professional Engineer in Australia.